

Downstream grain-size distribution of surficial bed material and its hydro-geomorphological significance in a large and regulated river: the Rhône River in its delta area (France)

Distribution granulométrique longitudinale des dépôts de fond superficiels et sa signification hydro-géomorphologique dans un grand fleuve chenalisé : le Rhône dans son aire deltaïque (France)

Gilles Arnaud-Fassetta*, David Quisserne*, Christelle Antonelli**

Abstract

This paper characterises the bed material in the two regulated distributaries of the Rhône Delta and examines the relationships among grain size, channel geometry, hydraulic conditions and distance from the coast. The Rhône River in its delta area is characterised by four bed-material types (cobble-pebble, sand, compact silt, mud). Sand beds are the most frequent. During low water flow, a small proportion of sand grains is mobilised by rolling. Sand transport capacity strongly increases at bankfull discharge, and bedload transport of sand is replaced by graded suspension. Finest cobble-pebble beds of the Grand Rhône are strictly mobile at bankfull discharge. Bed-material grain size is distinct between the Grand Rhône, which mainly transports cobble-pebble and coarse to medium sand, and the Petit Rhône, which predominantly transports medium to fine sand. Specific stream power differences, combined with local structural and geomorphological factors, explain this distinct bed-material grain size distribution in the two channels. An abrupt transition from cobble-pebble to sand beds occurs in the Grand Rhône 25 km upstream from the river mouth. On the Petit Rhône, a downstream fining occurs in the sand beds located in the lower section. At present, the Grand Rhône has a higher competence and a higher bed-material transport capacity than the Petit Rhône. High specific stream power explains the presence of numerous incised channel sections that create a bed-material *discontinuum*.

Key words: Rhône Delta, quantitative hydro-geomorphology, bed-material grain size, downstream fining.

Résumé

Cet article propose de caractériser les dépôts sédimentaires présents sur le fond actuel des deux bras du delta du Rhône. Le Rhône dans son delta est aujourd'hui caractérisé par quatre types de fond (galets, sables, limons compacts, vases). Les fonds sableux sont les plus fréquents ; les grains sont mobiles au contact du fond, mais seuls les grains les plus fins sont déplacés en faible quantité en période de basses eaux. La capacité de transport des sables s'accroît fortement lors du débit de pleins bords ; la suspension graduée se substitue alors au roulement pour devenir le processus de transport dominant. Seules les fractions les plus fines des stocks graveleux du Grand Rhône ne sont remobilisables lors du débit de pleins bords. La granularité des sédiments de fond diffère dans les deux bras du delta. Ce sont les galets et les sables grossiers à moyens qui caractérisent les fonds du Grand Rhône, alors que le Petit Rhône ne reçoit que des sables moyens à fins. Les puissances fluviales spécifiques, distinctes dans le Grand Rhône et le Petit Rhône, associées à l'influence des héritages géomorphologiques locaux, expliquent la granularité différenciée des fonds dans les deux bras. Une transition brutale entre les galets et les sables est mise en évidence 25 km en amont de l'embouchure du Grand Rhône ; dans le Petit Rhône, un affinement granulométrique se signale dans la section inférieure. Aujourd'hui, le Grand Rhône possède une plus forte compétence et une plus grande capacité de transport que le Petit Rhône. Les très fortes puissances spécifiques actuelles expliquent la présence de nombreuses sections de lit en incision nette, qui créent une discontinuité sédimentaire remarquable des dépôts de fond.

Mots clés : delta du Rhône, hydro-géomorphologie quantitative, granularité des dépôts de chenal, gradient granulométrique longitudinal.

* Équipe "Dynamique des Milieux et Risques", PRODIG (UMR 8586 CNRS), Université Denis-Diderot (Paris 7). CC 7001, 2 place Jussieu, F 75251 Paris cedex 05. E-mail: fassetta@paris7.jussieu.fr

** Équipe "Géomorphologie et Tectonique", CEREGE (UMR 6635 CNRS), Université Aix-Marseille 1, BP 80, F 13545 Aix-en-Provence cedex 04.

Version française abrégée

Au sortir du Petit Âge Glaciaire, le Bas-Rhône était encore une voie fluviale répuée pour transporter une charge sédimentaire abondante, dans un chenal dominé par les processus de remblaiement. À la fin du XIX^e siècle, diverses opérations de re-calibrage conduisent à sa métamorphose (contraction/incision) et à la modification des conditions hydrauliques, avec le renforcement de la compétence et des puissances spécifiques (Arnaud-Fassetta, 2003). Ces transformations hydro-géomorphologiques ont modifié les bilans sédimentaires et les processus de transport dans le chenal. Cette étude propose de faire le point sur l'état actuel du fond des deux bras du delta du Rhône (fig. 1 et 2), dont le rapport de débit est d'environ 9 pour 1. L'étude porte plus particulièrement sur la caractérisation sédimentologique des dépôts de chenal et sur les facteurs de contrôle du profil granulométrique longitudinal : géométrie du chenal, conditions hydrauliques (basses eaux, débit de pleins bords) et distance à la mer.

D'un point de vue méthodologique, la recherche est basée sur l'analyse combinée de 102 sites sélectionnés tous les kilomètres entre la diffluence et les deux bouches du Rhône. Sur chaque site, plusieurs types de données ont été recueillis : 1) sections en travers du chenal, levées par la CNR ; 2) données hydrologiques (débit, pente des lignes d'eau) fournies également par la CNR ; 3) échantillons sédimentaires et aqueux collectés en scaphandre autonome par G. Arnaud-Fassetta et D. Quisserne durant la période de basses eaux de juillet et août 1999 (fig. 3), complétés par deux carotages sédimentaires sous-aquatiques réalisés par M. Guillemard et G. Arnaud-Fassetta ; 4) granularité des dépôts de fond, analysée par comptage (galets) ou par granulométrie laser (sables, limons, argiles), et exploitation des résultats (grain médian, diagramme de Passega, courbe à ordonnées de probabilité de Visser) (D. Quisserne) ; 5) identification de la macrofaune benthique (P. Freydet et D. Quisserne) ; 6) mesure du taux de salinité pour la cartographie du coin salé au moment du prélèvement (D. Jézéquel et D. Quisserne) ; 7) calcul des paramètres hydrauliques : compétence, puissance spécifique, force tractrice et puissance critiques, capacité de transport (G. Arnaud-Fassetta).

Les résultats montrent que les bras du delta du Rhône sont aujourd'hui caractérisés par quatre types de fond : fonds à galets, fonds sableux, fonds à limons compacts et fonds vaseux (tab. 2). Les fonds sableux (photos 1C et 1D) sont les plus fréquents ; ils constituent respectivement 59 % et 79 % des fonds dans le Grand Rhône et le Petit Rhône (tab. 2). Leur médiane granulométrique (D_{50}) varie de 0,65 mm à 0,20 mm (sables moyens à fins) (fig. 4B et 4C) ; les fonds du Grand Rhône sont caractérisés par des sables plus grossiers (D_{50} dominant = 0,55-0,50 mm) que ceux du Petit Rhône (D_{50} dominant = 0,45-0,40 mm). Deux modes de transport principaux participent à leur déplacement (fig. 5) : la suspension graduée (à hauteur de 35-54 % ; fig. 6) et le roulement plus ou moins associé à la suspension graduée (34-52 % ; fig. 6). Ce dernier mode de transport "combiné" est plus fréquent dans le Grand Rhône. Les galets, qui cou-

vrent 27 % du linéaire fluvial, affichent une médiane granulométrique (D_{50}) comprise entre 80 mm et 30 mm (fig. 4A) ; le processus de transport est le roulement (fig. 5). Ils ne sont présents que dans les secteurs de haute énergie du Grand Rhône, en amont du kilomètre 25 (photos 1A et 1B) ; plus en aval, ils disparaissent pour laisser place à des fonds sableux dominants. La zone source de ces galets est discutée : apport récent du Rhône ? remaniement du cailloutis durancien pléistocène ? remaniement des cordons littoraux holocènes ? La structure de certains dépôts (galets sur sables), observée en plongée, atteste que la non-mobilité des galets n'est pas une certitude ; les plus petits d'entre eux pourraient bien avoir été re-mobilisés lors des dernières fortes crues du fleuve, ce qui, du reste, est confirmé par les estimations de la compétence et des puissances critiques proposées dans cet article (tab. 3). Les limons compacts (12-17 %), essentiellement localisés dans les mouilles, affichent des médianes granulométriques (D_{50}) comprises entre 0,08 mm et 0,01 mm (fig. 4D et 4E). Surtout, leur faciès de limons massifs ou finement laminés, compacts, à forte bioturbation et à faunes typiquement palustres, indique qu'il s'agit de formations fossiles (plaine d'inondation), exhumées, dans lesquelles s'emboîte l'enveloppe du lit fluvial actuel (photos 1E et 1F). Ils sont les témoins de secteurs où le plancher alluvial du Rhône est en incision nette. Enfin, les vases (2-4 %) sont constituées de limons argileux plus ou moins sableux (D_{50} = 0,077-0,019 mm ; fig. 4F et 4G) et organiques. Strictement observées dans les derniers kilomètres du fleuve, leur présence s'explique par l'incursion du coin salé qui joue un rôle déterminant dans la floculation des argiles sur le fond du chenal fluvial.

Le profil granulométrique longitudinal du fond des chenaux du delta du Rhône (fig. 7 et 8) montre que la taille maximale (D_{90}) et médiane (D_{50}) du matériel décroît de la diffluence (Grand Rhône : D_{90} = 57,60 mm, D_{50} = 34,00 mm ; Petit Rhône : D_{90} = 0,78 mm, D_{50} = 0,63 mm) jusqu'aux embouchures (Grand Rhône : D_{90} = 0,63 mm, D_{50} = 0,55 mm ; Petit Rhône : D_{90} = 0,48 mm, D_{50} = 0,43 mm). Ce schéma est conforme à la décroissance amont-aval des puissances fluviales. Par ailleurs, une transition brutale entre les galets et les sables est mise en évidence 25 km en amont de l'embouchure du Grand Rhône (fig. 7). Elle s'explique par la conjonction de trois facteurs : structural (affleurement du cailloutis durancien pléistocène ou des cordons littoraux à galets holocènes), géomorphologique (réduction locale de la pente du lit, effet de seuil) et hydraulique (réduction des puissances spécifiques). Ainsi, en aval du kilomètre 25, la médiane granulométrique (D_{50}) décroît très rapidement de 70-45 mm à 0,65 mm en quelques kilomètres seulement. Dans le Petit Rhône, le gradient granulométrique, moins brutal, est globalement décroissant de la diffluence jusqu'à l'embouchure (fig. 8). Il est lié à un transport sélectif des sables et à l'abandon des plus grossiers d'entre eux dans les secteurs de basse énergie ; dans la partie aval s'ajoutent l'effet de la forte sinuosité et l'influence de la décroissance graduelle des puissances fluviales. Au total, les possibilités de piégeage du matériel sableux dans le lit du Petit Rhône sont nombreuses, ce qui

peut être considéré comme un préjudice à la bonne alimentation sédimentaire des plages littorales plus en aval.

Les relations qui lient la granularité aux conditions hydrodynamiques (modes de transport, hydraulique du chenal) sont examinées. Concernant le matériel sableux, les grains sont mobiles au contact du fond, mais seuls les plus fins d'entre eux sont déplacés, en faible quantité, en période de basses eaux (tab. 3). Ceci vaut surtout pour le Grand Rhône ($Q \approx 900 \text{ m}^3 \text{ s}^{-1}$; $D_{50} = 0,50\text{-}0,35 \text{ mm}$; $i_b = 0,005\text{-}0,002 \text{ kg m}^{-1} \text{ s}^{-1}$) car le transport reste insignifiant dans le Petit Rhône ($Q \approx 100 \text{ m}^3 \text{ s}^{-1}$; $D_{50} = 0,08\text{-}0,05 \text{ mm}$; $i_b = 0,00005 \text{ kg m}^{-1} \text{ s}^{-1}$) (tab. 3 et fig. 9). Quoi qu'il en soit, le mode de transport des sables est alors dominé par le roulement. La capacité de transport du matériel sableux s'accroît fortement lors du débit de pleins bords; la suspension graduée se substitue alors au roulement pour devenir le processus de transport dominant. Concernant les galets du Grand Rhône, ils ne sont re-mobilisables qu'une fois atteint le débit de pleins bords. Les puissances critiques, en général très élevées ($180,80\text{-}59,82 \text{ W m}^{-2}$), font que la majorité d'entre eux reste immobile (fig. 9): seuls les plus petits galets ($D_5 = 10\text{-}15 \text{ mm}$) sont remobilisables mais en quantité réduite ($Q \approx 5400 \text{ m}^3 \text{ s}^{-1}$; $D_5 = 10\text{-}15 \text{ mm}$; $i_b = 0,343\text{-}0,091 \text{ kg m}^{-1} \text{ s}^{-1}$). Aujourd'hui, le Grand Rhône possède une plus forte compétence et une plus grande capacité de transport que le Petit Rhône (respectivement +255 % et +1750-1880 % pour la charge sableuse lors du débit à pleins bords). Les très fortes puissances spécifiques expliquent la présence de nombreuses sections de lit en incision nette, qui créent une discontinuité sédimentaire remarquable sur le fond actuel des deux bras du delta.

Introduction

In a deltaic plain, only part of the total sediment load supplied by the river directly joins the coastal fringe during hydrological events. A significant proportion of the sediment load temporally accumulates in the river in which many processes control the temporal and spatial grain size distribution. Furthermore, river morphology strongly depends on both transport capacity of the water flow and on volume and grain size of the sediment supplied. Channel-pattern adjustments over time are linked to changes in hydro-geomorphological conditions that were expressed by E.W. Lane (1955) in terms of a proportional relationship:

$$Q S \propto Q_s D_s \quad (1)$$

where Q = water discharge, S = channel slope, Q_s = sediment discharge and D_s = a characteristic grain size of the river-bed material.

In the Rhône Delta, channel morphology and sediment dynamics have been altered since the end of the Little Ice Age by a series of climatic and societal factors. Channel narrowing and riverbed incision were a response to decreased flood frequency and sediment yield. In addition, channelisation projects during the late 19th century increased bankfull discharge and specific stream power (Arnaud-Fassetta, 2003). Conse-

quently, dramatic sediment yield decrease of the Rhône River has been identified as one of the main causes of accelerated beach erosion of the delta (Suarez and Provansal, 1998).

Examples of downstream changes in grain size on gravel and sandy rivers have been well documented in recent years (Werrity, 1992; Ferguson *et al.*, 1996; Hoey and Bluck, 1999; Rice, 1999; Doyle and Shields, 2000). In the case of the Rhône Delta, the study by D. Quisserne (2000) highlighted downstream changes in bed-material grain size in the two Rhône channels. Four reasons justify undertaking this type of research. First, several investigations have been interested in sediment yield brought by the Rhône River to the Mediterranean Sea (Surrell, 1847; Pardé, 1925; Van Straaten, 1959; Pauc, 1976; Pont *et al.*, 2002), but these works highlighted the relative paucity of studies characterising the nature and dynamics of bed material in the Rhône Delta. Second, downstream changes in grain size have been mentioned in several studies (Carrio, 1988; Dugas, 1989; Pont, 1992; Roditis, 1993), but have seldom been described in any detail or explained. Third, several studies on sedimentation processes during rare flooding events focused mainly on the floodplain (Arnaud-Fassetta, 1996, 2000; Hensel *et al.*, 1999), but no studies have been carried out on the in-channel deposits. Fourth, most work pertaining to in-channel dynamics was supported by stationary, discontinuous measures recorded at only a few sites (Carrio, 1988; Pont *et al.*, 2002). These earlier studies have thus not taken account of the spatial variability of bed-material grain size, nor evaluated the morphodynamic specificities of each Rhône Delta distributary.

The aim of our investigation is (1) to discriminate between bed-material types in the two channels of the Rhône Delta in terms of sedimentology, and (2) to analyse factors controlling the longitudinal profile of bed material in terms of channel geomorphology, hydraulic conditions and distance from the river mouth.

Major attributes of the Rhône River in its delta

The Rhône River drains a large temperate catchment of $\sim 97,800 \text{ km}^2$ and discharges on the southern coast of France in the Mediterranean Sea, a microtidal marine basin (fig. 1). Its delta is predominantly a high destructive wave-dominated one resulting from a gradual, restricted sediment supply. The total area of the delta is $\sim 1,740 \text{ km}^2$, of which 72% is floodplain (ancient and modern), 23% is permanent lagoons and ponds, and 5% is coastal environments. Since the completion of river embankments (late 19th century), the active floodplain account for only 5% of the total delta plain.

At the head of the delta, at Fourques, the Rhône River divides into two distributaries (fig. 2). The Grand Rhône is the main channel, with 85-90% of the total discharge. Its course is 50 km long and straight to moderately sinuous (1.0 to 1.3). It exhibits a pool-riffle bed topography, producing a variation in the longitudinal bed slope. According to the classification of R. Kellerhalls *et al.* (1976), the Grand Rhône channel type may be defined as $[a_0, b_1, c_4]$ upstream of

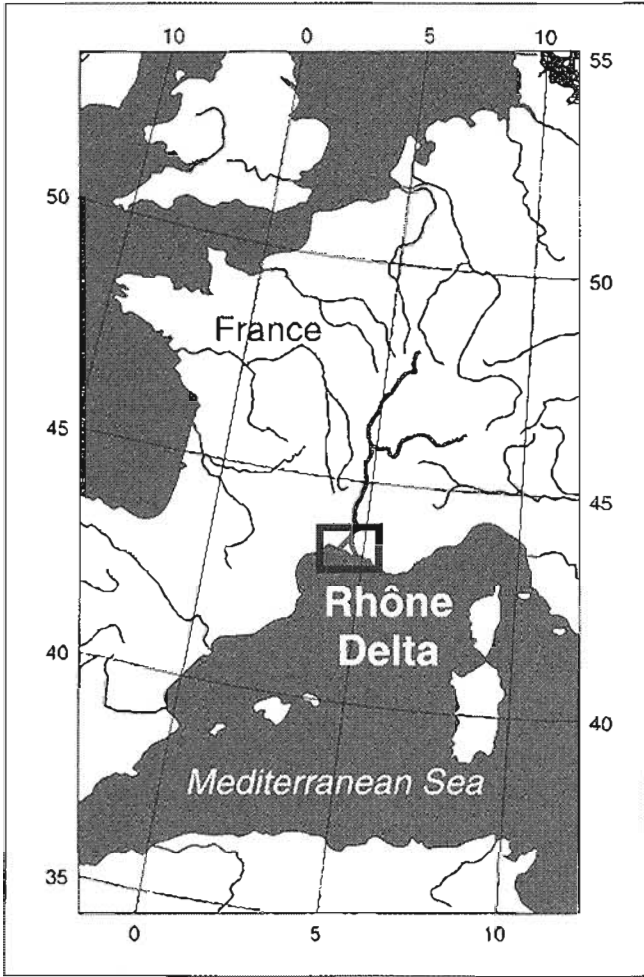


Fig. 1 – Location map of the Rhône Delta.

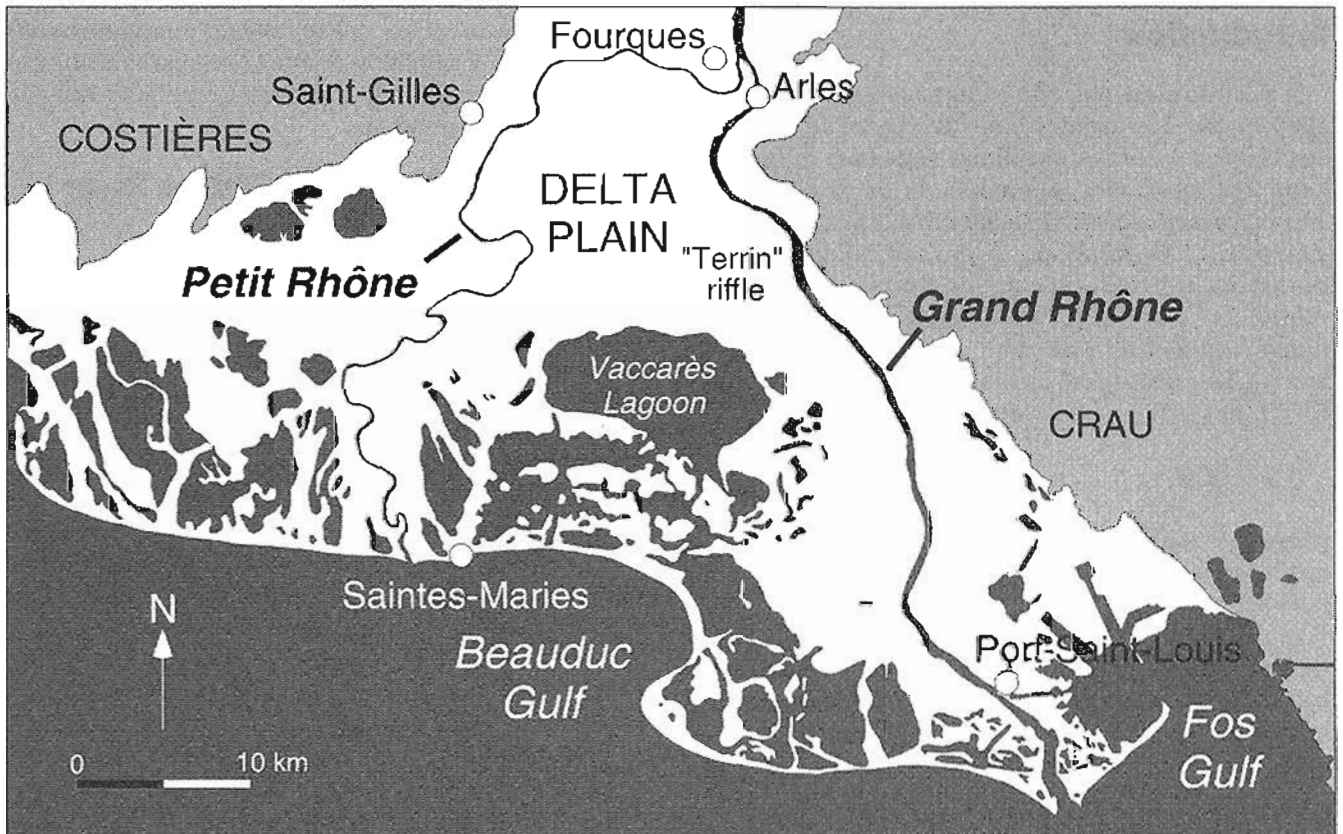
Fig. 1 – Carte de localisation du delta du Rhône.

Arles, and as $[a_1, b_0, c_1 \text{ or } c_2]$ type downstream. In contrast, the Petit Rhône (60 km long) drains 10-15% of the total Rhône discharge since modern channel regulation. It is moderately sinuous (1.35) until 35 km from the sea, and sinuous (1.7) further downstream. It may be defined as a $[a_3, b_1, c_1, c_2 \text{ or } c_3]$ channel type upstream of Saint-Gilles, and as a $[a_4, b_0, c_1, c_2 \text{ or } c_3]$ type downstream (Kellerhalls *et al.*, 1976). In detail, bed topography is represented by successive riffle-pool sequences, and rare pointbars indicate that very few parts of the river are undergoing meander migration as a result of channel embankment.

The hydrological regime of the lower Rhône River varies from a dominant nival-pluvial type to a pluvial Mediterranean type with nival supplies. At the Beaucaire water-gauge station, its mean annual discharge is $1,701 \text{ m}^3 \text{ s}^{-1}$. Water discharge is characterised by a strong intra- and inter-annual variability (tab. 1) because of various influences (*i.e.*, glacial, nival, pluvial) in the river basin (Pardé, 1925). In the delta, salt-wedge intrusion occurs in both distributary channels when the discharge is lower than $\sim 1,000 \text{ m}^3 \text{ s}^{-1}$ at Beaucaire (CNR data). The salt wedge can be considered as a main cause of clay sedimentation near the river mouth (Savey *et al.*, 1971). During field measurements of July-August 1999, the salt wedge was located respectively 13 km

Fig. 2 – Map of the Rhône Delta.

Fig. 2 – Carte du delta du Rhône.



100-year R. I. flood	11,640 (May 1856)
80-year R. I. flood	10,981 (Jan. 1994)
50-year R. I. flood	9,800 (Oct. 1993)
30-year R. I. flood	9,400 (Nov. 1994)
10-year R. I. flood	8,300
2-year R. I. flood	6,000
1-year R. I. flood	4,200
Mean annual discharge	1,701
Semi-permanent discharge	1,460
Low water discharge	580
Minimum low water discharge	320 (Oct. 1921)

Table 1 – Selected characteristic discharges of the lower Rhône River at the Beaucaire station, 60.5 km upstream of the Grand Rhône river mouth (CNR data). Values are in percentages.

Tableau 1 – Quelques débits caractéristiques du Bas-Rhône à la station de Beaucaire, 60,5 km en amont de l'embouchure du Grand Rhône (données CNR). Les valeurs de débit sont exprimées en pourcentages.

(Grand Rhône) and 8 km (Petit Rhône) upstream from the river mouth, with a discharge of $\sim 1,000 \text{ m}^3 \text{ s}^{-1}$ at Beaucaire. The present-day sediment mass carried by the Rhône River is estimated in the delta at an average of $9\text{-}10 \times 10^6 \text{ t yr}^{-1}$, with variations from $2.6 \times 10^6 \text{ t yr}^{-1}$ to $27 \times 10^6 \text{ t yr}^{-1}$ (Antonelli, 2002). In addition, the sediment yield of the Rhône River has decreased by 70-80% since the first part of the 19th century, highlighting the importance of climatic and anthropogenic modifications at the river basin scale.

Material and methods

Characterisation of bed material in the two river channels of the Rhône Delta, and its relations with channel geometry, hydraulic conditions and distance from the sea, have been

analysed on the basis of field survey, sedimentological analysis and hydraulic measurements.

Field survey procedures

The survey covered a channel distance of 110 km along the two channels in the Rhône Delta. A systematic study was carried out between the Rhône diffuence and the two river mouths. One hundred and two field sites were selected at one kilometre intervals in the Grand Rhône (44 field sites) and the Petit Rhône (58 field sites). The surveys were carried out with a 5 m-long inflatable boat equipped with a digital reading ultrasonic echo-sounder EAGLE Ultra Classic. In obtaining position location in the channel at maximum depth, measurement error was less than $\pm 0.1 \text{ m}$. Two scuba-diving surveys were undertaken by G. Arnaud-Fassetta and D. Quisserne at low water flow, respectively from 22 July to 24 July 1999 on the Petit Rhône and from 29 August to 30 August 1999 on the Grand Rhône. Both were undertaken under the same hydroclimatic conditions: strong NW wind (*i.e.*, the "Mistral"), low W-NW swell and average river discharge of $961\text{-}1,095 \text{ m}^3 \text{ s}^{-1}$ at the Beaucaire water-gauge station. The hydrological regime during the study period is presented on figure 3.

One hundred and two samples of bed material were collected with polythene bags at the deepest point of each channel cross-section surveyed. Each sampling procedure was preceded by scuba-diving reconnaissance in an area of about 100 m^2 so as to select the best, representative site. For sandy material, the total weight of the collected samples was 1-2 kg. For the cobble-pebble material, M.A. Church *et al.* (1987) recommended that the weight of the coarsest particle not exceed 1% of total sample weight. In the Rhône River, this would have required to collect samples of 1-2 tons. Thus, only samples of 100-250 kg were collected and the coarsest particle weight never exceeded 6% of the total sample. In addition, two short cores (1 m in length) were extracted from the alluvial floor of the Petit Rhône, 53 km upstream of the mouth, with a 8 cm-diameter core sampler in view of determining precisely cohesion and structure of both the sand and silt deposits.

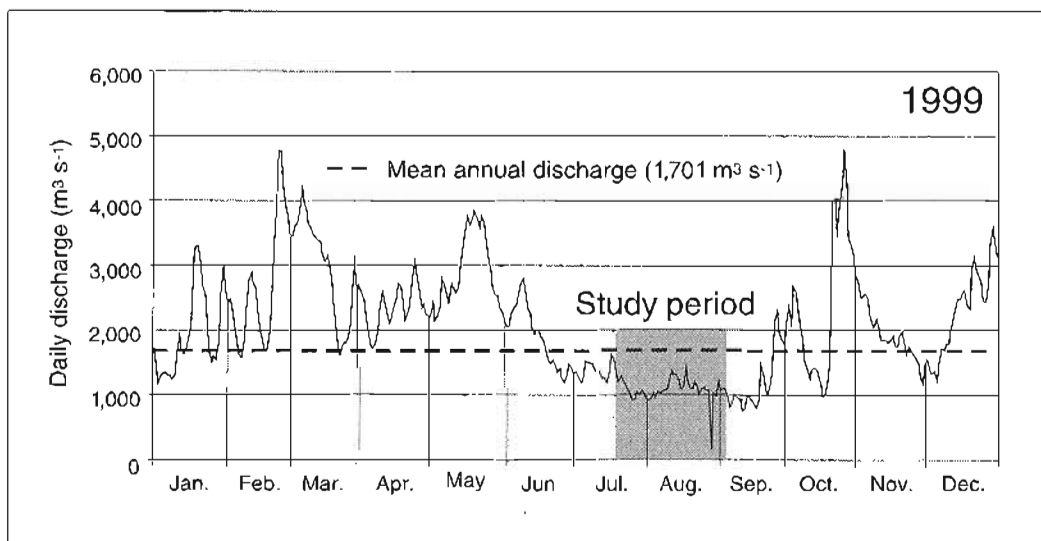


Fig. 3 – Flood hydrograph for the study period. Values are based on gauging measurements at the Beaucaire station (CNR data).

Fig. 3 – Hydrogramme de crue de la période étudiée. Les débits ont été collectés à la station de Beaucaire (données CNR).

Characterisation of sediment facies and bed-material grain size

Samples were analysed (University of Paris 7) using standard laboratory techniques (Folk, 1980). Sediment facies were identified on the basis of colour, lithology, structure (observed both *in situ* and in the lab when possible), sediment cohesion and fauna. For grain-size characterisation, the <1 mm fraction was analysed by laser granulometre COULTER COUNTER LS 100 and the >1 mm fraction was analysed using dry-sieving technique (AFNOR standard). For each sample, standard deviation (σ) and skewness (sk_1) were calculated using the method proposed by R.L. Folk and W.C. Ward (1957). Grain-size data were characterised by computing D_{50} = median bed-material grain size. As indicated by M.W. Doyle and F.D. Shields Jr. (2000), D_{50} best represents grain-size distribution, and thus was used for the analyses.

First, D_{50} was plotted against distance upstream of the river mouth, yielding profiles of median bed-material grain size for each distributary of the Rhône Delta. It was in some cases replaced by D_{90} = 90th percentile or D_5 = 5th percentile, for highlighting downstream fining of coarse sediment in the Grand and Petit Rhône.

Second, D_{50} was plotted against D_{99} = maximum bed-material grain size on a log-log diagram as described by R. Passega (1957), and referred here as CM diagram. For each sample, plotting of D_{50} and D_{99} on the CM diagram yields precise description of bed-material grain size as related to associated transport processes. Three types of sediment transport by tractive currents were distinguished: (1) rolling of particles (cobbles and pebbles) on the alluvial floor, (2) saltation of medium and fine sands near the channel floor, (3) suspension of fine sand and silty sand situated at the top of the water column and sometimes near the channel floor. On the CM diagram, the *NO* segment corresponds to coarse rolling particles, the *PQ-QR* segments represent graded suspension or mixed fine rolling particles and graded suspension, and the *RS* segment relates to uniform suspension. In their study, J.P. Bravard and J.L. Peiry (1999) argued that the position of the *RS* segment in the CM diagram depends on turbulence of the reach and that the segment can shift vertically in relation to stream power variation. This approach has been adopted in this study. Therefore, the *RS* segment was divided into two parts: the *R'S'* segment corresponds to a mixture of uniform suspension and graded suspension, while *RS* relates to uniform suspension (Arnaud-Fassetta, 1998). Quantification of each mode of sediment transport was made using log-probability grain-size distribution curves (Visher, 1969). This method proposes that each cumulative curve comprises a number of straight-line segments of different slope separated by sharp "breaks". The straight-line segments are interpreted as truncated log-Gaussian subpopulations. Each log-Gaussian subpopulation recognized is related to a mode of sediment transport: rolling (coarsest subpopula-

tion), saltation (or graded suspension of Passega; intermediate subpopulation), suspension (*i.e.*, uniform suspension of Passega; finest subpopulation).

Third, D_{50} is used in several hydraulic calculations, including bed-material transport capacity and critical stream power.

Hydraulic calculations

One hundred and two channel cross-sectional areas were obtained from the Compagnie Nationale du Rhône (CNR). These cross-sections were surveyed perpendicular to the assumed flow direction of the Petit Rhône and the Grand Rhône, respectively in 1994 and 1999. Several hydraulic parameters (stream power, bed shear stress, transport capacity) were calculated at the University of Paris 7 for low water conditions (*i.e.*, discharge during the study period) and for bankfull discharge.

The specific stream power (ω) was calculated using the R.A. Bagnold (1966) equation:

$$\omega \text{ (W m}^{-2}\text{)} = (\rho_w g Q S) W^{-1} \quad (2)$$

where ρ_w = water density (kg m^{-3}), g = gravitational acceleration (m s^{-2}) and W = channel width (m). Discharge values during field measurements (Q_{LF}) and at bankfull discharge ($Q_b \propto Q_2 \propto 6,000 \text{ m}^3 \text{ s}^{-1}$ at Beaucaire) were obtained from the CNR.

Also, in the absence of direct measurements of bed-material transport, an alternative method of estimating bed-material transport was required (Gilvear and Bradley, 1997; Ham and Church, 2000). J.C. Bathurst *et al.* (1987), followed by B. Gomez and M. Church (1989), concluded that the stream power function of R.A. Bagnold (1980) performs best when predicting the bed-material transport capacity in sand-bed or in gravel-bed channels. In this study, bed-material transport capacity of the Rhône River is estimated using a revised R.A. Bagnold (1980) formula, which is more appropriate for sand and gravel transport; the specific bed-material transport capacity (i_b) is given in Y. Martin and M. Church (2000) by:

$$i_b \text{ (kg m}^{-1} \text{ s}^{-1}\text{)} = (\omega - \omega_0)^{3/2} (D^{1/4} d^{-1}) [1 (\rho_r^{1/2} g^{1/4})^{-1}] \quad (3)$$

where ω_0 = critical stream power (W m^{-2}) for bed-material transport, D = characteristic particle size usually denoted in

Table 2 – Lithologic nature of alluvial floor in the Grand Rhône and Petit Rhône.

Tableau 2 – Nature des fonds du Grand Rhône et du Petit Rhône.

<i>Grand Rhône</i>	Cobble-pebble	Sand	Ancient silt	Mouth mud	Total
n	12	26	5	1	44
%	27	59	12	2	100
<i>Petit Rhône</i>	Cobble-pebble	Sand	Ancient silt	Mouth mud	Total
n	0	46	10	2	58
%	0	79	17	4	100

mixtures by D_{50} (m). d = mean depth (m) and ρ_r = submerged sediment density (kg m^{-3}), defined by:

$$\rho_r = \rho_s - \rho_w \quad (4)$$

where ρ_s = sediment density (kg m^{-3}). Moreover, critical stream power (ω_0) is defined by the R.A. Bagnold (1980) equation, expressed in Y. Martin and M. Church (2000) as:

$$\omega_0 (\text{W m}^{-2}) = 5.75 [0.04 (\gamma_s - \gamma_w) \rho_w]^{3/2} (g \rho_w^{-1})^{1/2} (D)^{3/2} \log(12d D^{-1}) \quad (5)$$

where γ_s = specific gravity of sediment and γ_w = specific gravity of water.

The critical conditions for initiation of bed-material movement were calculated using the A. Shields (1936) equation:

$$\theta_c = \tau_c [g (\rho_s - \rho_w) D]^{-1} \quad (6)$$

where θ_c = dimensionless critical shear stress and τ_c = critical shear stress (N m^{-2}) needed to initiate movement, which depends principally on grain size, according to the equations:

$$\tau_c = 1.66 D \text{ (sand river beds)} \quad (7)$$

and

$$\tau_c = D \text{ (cobble-pebble river beds)} \quad (8)$$

In addition, θ_c was related to a particle Reynolds number (Re_s). It can be approximately defined by the equation by D. Knighton (1998):

$$Re_s \propto D \delta_0^{-1} \quad (9)$$

where δ_0 = thickness of the laminar sublayer (m).

Results

Bed-material types

The scuba surveys in the summer of 1999 allowed us to identify four different bed-material types in both channels of the Rhône Delta. Table 2 gives the respective proportion of each bed-material type. On the Grand Rhône, for a total of 44 field sites, 12% of the fluvial bed was characterised by cohesive sediments, essentially ancient floodplain silt. The cohesionless sediments (88%) were composed of cobble-pebble (27%), sand (59%) and mud at the mouth (2%). On the Petit Rhône, for a total of 58 field sites, the percentage of cohesive sediments was higher, due to the presence of ancient silty floodplain deposits (17%). Sand (79%) is the most frequent bed-material type. At the river mouths, mud (4%) is most abundant, and cobble-pebble beds are rare. In conclusion, cobble-pebble, sand and silt dominate but in varying proportions depending on the different morphological units. The bed-material types are described in the following sections.

Cobble-pebble beds

The coarsest bed material of the Rhône River in the delta is restricted to the deepest part of the channel section (photo 1A). Such coarse deposits are abundant only in the upper Grand Rhône (*i.e.*, to 25 km from the sea) where energy slope, flow velocity and specific stream power are high. Petrographic analysis indicates a typical Durancian suite of quartzite, "verrucano", radiolarite, green rock, granite, sandstone and limestone. At the "Terrin" riffle, the Pleistocene alluvial deposits of the Durance River (*i.e.*, the "Crau") may be a possible source of channel cobble-pebble deposits. It is not excluded, however, that cobble-pebble deposits correspond to the reworking of Holocene marine shingle bars (L'Homer, 1987; Vella, oral comm.). Especially below Arles (42 km upstream of the mouth), a small but original part of the cobble-pebble beds corresponds to coarse and rounded shards derived from the destruction of Roman rubbish dump deposits and their displacement down the Grand Rhône (photo 1B). The remainder of the cobble-pebble fraction are of stone block origin, resulting from the destruction of submersible dikes by large flood events. Most of cobble-pebble deposits have an open framework (lacking matrix completely), are imbricated and exhibit massive structure. In some cases, cobble-pebble deposits are clast-supported and associated with medium and fine sand matrix. Further downstream (25 km upstream from the river mouth), river sands are buried by some cobbles and pebbles. It is necessary to distinguish between cobble-pebble deposits displaced by fluvial process and those of autochthonous Pleistocene, non reworked bed-substrate origin; the latter usually appears as cohesive deposits, with calcareous cement or argillaceous matrix. Median grain size (D_{50}) ranges from 80 mm to 30 mm, but most deposits (85%) correspond to very well to moderately sorted ($0.26 < \sigma_1 < 0.73$) coarse pebbles with a median grain size of 60-30 mm (fig. 4A) and variable asymmetry with sk_1 between 0.33 and -0.40. The CM diagram (fig. 5) indicates that dominant transport process displacing cobbles and pebbles is by rolling (*NO* segment).

Sand beds

Cohesionless quartz-lithic sand appears in both riffle and pool sections (photos 1C and 1D). They show mostly small sigmoidal and asymmetric ridges (height = 0.1-0.2 m; ridge spacing = 0.5-1 m) with a dune front oriented perpendicularly to the current. Sedimentary structure in the sand beds include cross bedding. In the upper and median sections of the Rhône River in its delta, sand beds are rich in permanent freshwater fauna adapted to high energy channel flows, particularly *Corbicula fluminea*, *Dreissena polymorpha* and *Neritina fluviatilis* (photo 1F). Because of possible salt wedge incursions in the river channels, *Corbicula fluminea* disappears respectively at 22 km and 25 km upstream of the mouth of the Grand Rhône and Petit Rhône. Near the river mouth, sands contain marine species (*Cerastoderma glaucum*, *Tellina planata*) associated with a downstream decrease of freshwater species (*Dreissena polymorpha*). The median grain size (D_{50}) ranges from 0.65 mm to 0.20 mm thus indi-

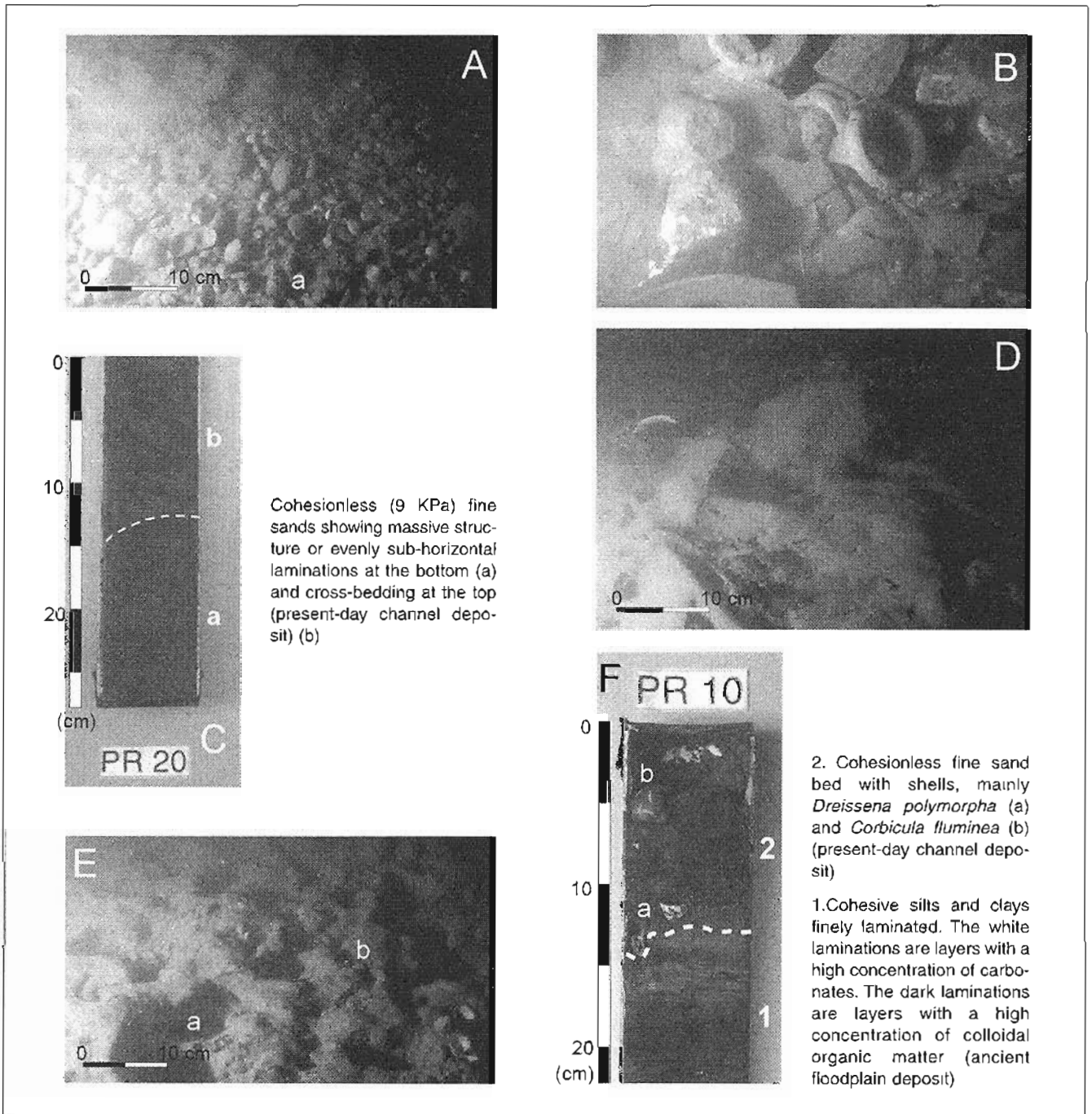


Photo 1 – Bed-material types characteristic of the Rhône River in its delta. A: cobble-pebble bed in the Grand Rhône; note presence of (a) *Corbicula fluminea* mixed with bed material (photo by M. Guillemard); B: view of the channel bottom immediately downstream from Arles; the rounded shards layer derived from the destruction of Roman (Low Empire) rubbish dump deposits in the Grand Rhône (photo by L. Long); C: sediment core showing grain size and sedimentary structures in the sand channel deposit (photo by G. Arnaud-Fassetta); D: sand bed in the Petit Rhône, flow from left to right (photo by M. Guillemard); E: view of old compact silts on the incised alluvial floor of the Petit Rhône; note that cavitation processes caused scour of (a) small subcircular depressions used as shelter by channel bottom fauna, especially (b) *Corbicula fluminea* (photo by M. Guillemard); F: sediment core showing present-day channel material covering ancient floodplain deposit in channel floor of the Petit Rhône (photo by G. Arnaud-Fassetta).

Photo 1 – Types de sédiment présents au fond des chenaux du delta du Rhône. A : accumulation de petits galets sur le fond du Grand Rhône; noter la présence de *Corbicula fluminea* (a) associé au matériel de fond (cliché M. Guillemard ; B : le fond du chenal du Grand Rhône immédiatement en aval de la ville d'Arles ; la couche de tessons émoussés provient du remaniement d'un dépôt de débris du Bas Empire situé en bordure du chenal (cliché L. Long) ; C : carotte sédimentaire montrant la granularité et la structure des sables de fond de chenal (cliché G. Arnaud-Fassetta) ; D : accumulation sableuse sur le fond du chenal du Petit Rhône ; l'écoulement fluvial se fait de la gauche vers la droite (cliché M. Guillemard) ; E : limons compacts (ancienne plaine d'inondation) exhumés sur le fond du chenal en cours d'incision du Petit Rhône ; un processus de cavitation est à l'origine du creusement de petites dépressions sub-circulaires (a) qui servent d'abri pour les faunes vivant sur le fond du chenal, *Corbicula fluminea* (b) en particulier (cliché M. Guillemard ; F : carotte sédimentaire prélevée sur le fond du Petit Rhône, qui révèle la présence d'une mince couche de sables fins recouvrant les anciens dépôts limoneux de plaine d'inondation (cliché G. Arnaud-Fassetta).

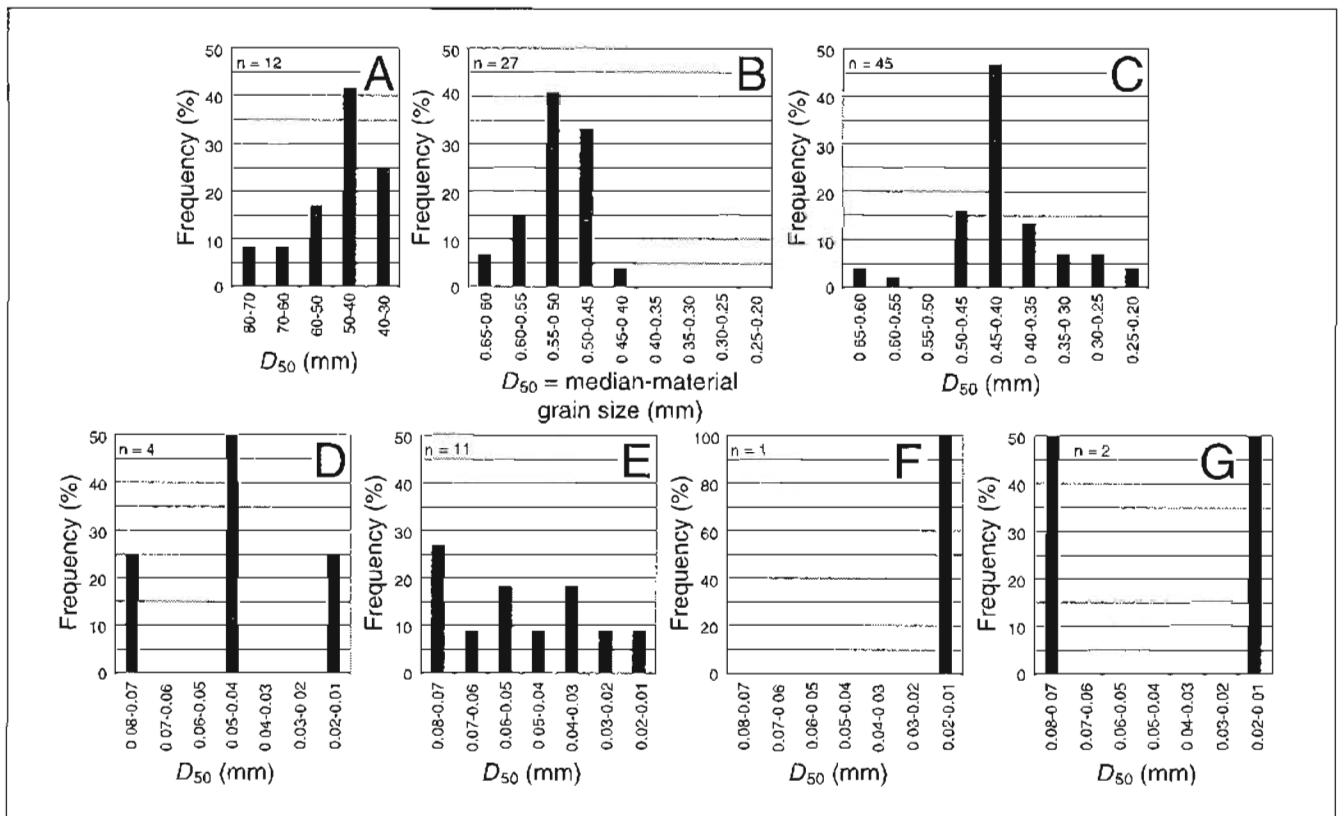


Fig. 4 – Median grain-size frequencies of bed-material type in the Rhône Delta. A: cobble-pebble beds of the Grand Rhône; B: sand beds of the Grand Rhône; C: sand beds of the Petit Rhône; D: compact silt beds of the Grand Rhône; E: compact silt beds of the Petit Rhône; F: river mouth mud bed in the Grand Rhône; G: river mouth mud beds in the Petit Rhône.

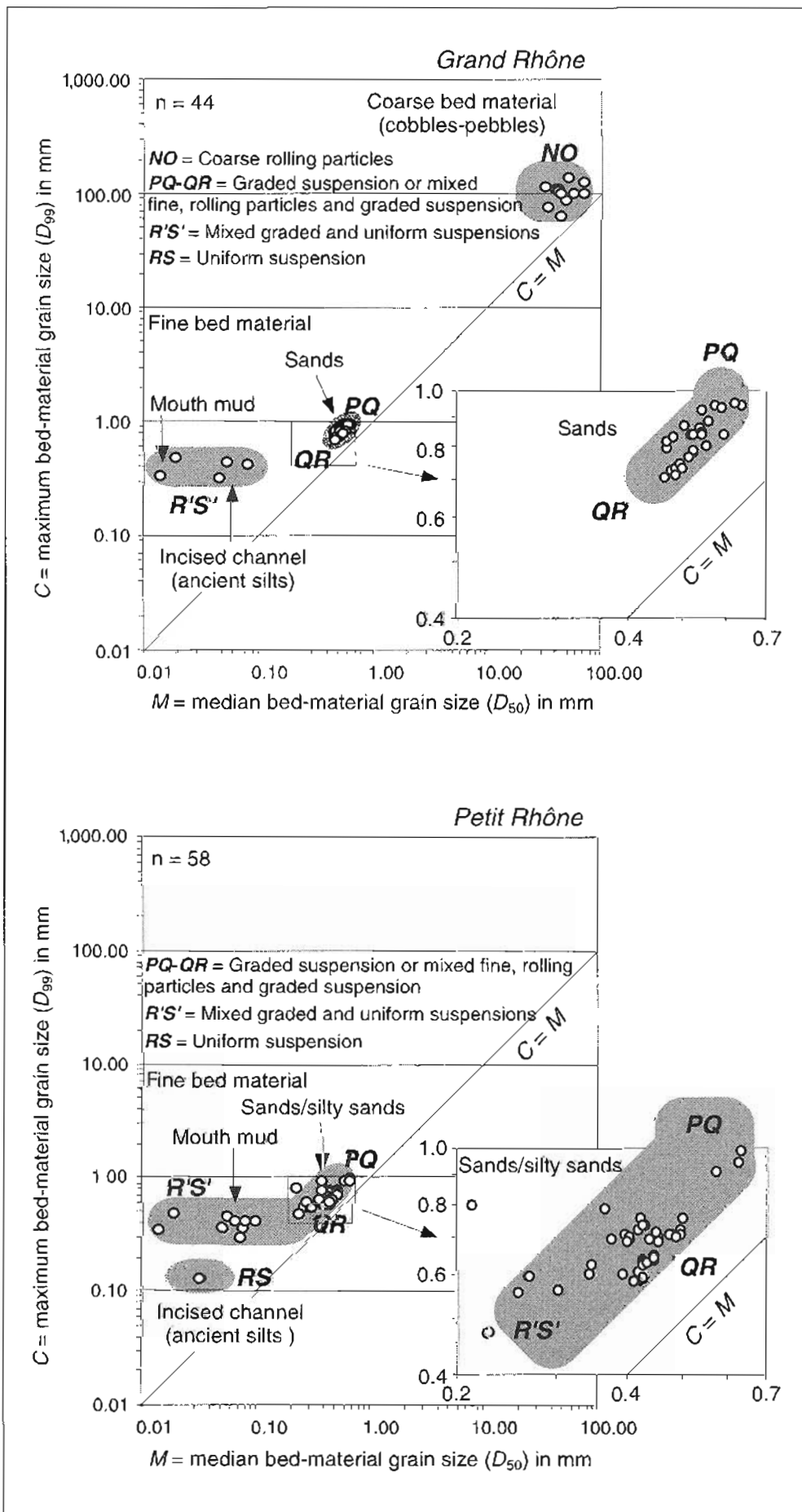
Fig. 4 – Distribution du grain médian (exprimée en fréquences) par type de fond des chenaux du Rhône. A : fonds à galets du Grand Rhône ; B : fonds sableux du Grand Rhône ; C : fonds sableux du Petit Rhône ; D : limons compacts constituant les fonds du Grand Rhône ; E : limons compacts constituant les fonds du Petit Rhône ; F : fonds vaseux de l'embouchure du Grand Rhône ; G : fonds vaseux de l'embouchure du Petit Rhône.

cating the sediments are coarse to fine sand (fig. 4B and 4C). Variations of D_{50} are more important in the Petit Rhône (0.65-0.20 mm) than in the Grand Rhône (0.65-0.40 mm). The D_{50} value is generally coarser in the Grand Rhône, with a dominant median grain size of 0.55-0.50 mm, than in the Petit Rhône, with a median grain size of 0.45-0.40 mm. Sand deposits are well to moderately sorted ($0.33 < \sigma_1 < 0.84$), with a typical high positive asymmetry ($0.25 < sk_1 < 0.77$). Their silt-clay content is about 2-3%, in response to the high energy channel environment. Only fine sands of the Petit Rhône are characterised by poor to very poor sorting ($1.39 < \sigma_1 < 2.84$) because of a strong increase in fine silt content ($0.73 < sk_1 < 0.90$) in low energy channel environments. The CM diagram of sand channel deposits is shown in figure 5. This indicates that most riverbed sand in the Rhône Delta corresponds to graded suspension or a mixture of rolling and graded suspension (PQ-QR segments). The fine sand position of the Petit Rhône on the R'S' segment results from a mixture of graded suspension and uniform suspension depo-

sition in low energy zones of the channel during flood recession. Discrimination of transport modes by the G.S. Visher (1969) method confirms this hypothesis (fig. 6). Graded suspension (mean 35-54%) or mixed rolling and graded suspension (mean 34-52%) represent the main transport processes of the sand fraction in both distributaries of the Rhône Delta. However, the percentage of sediment from each transport process is variable as a function of channel geometry and dynamics, as shown in figure 6. It is also noted that mixed rolling and graded suspension are more frequent in the Grand Rhône than in the Petit Rhône, dominated by graded suspension.

Compact silts

About 70% to 80% of compact silt beds, respectively, occur in pool sections of the Grand Rhône and Petit Rhône channels. This facies consists of massively structured sandy silt and heavily bioturbated silt, rich in organic matter (photo 1E). The silts contain a large suite of palustrine fauna, including *Limnea peregra*, *Planorbis carinatus*, *Valvata piscinalis* and *Paludetrina acuta*. Grain size analysis shows the compact silts [median grain size (D_{50}) = 0.08-0.01 mm; fig. 4D and 4E] to be very poorly sorted ($1.81 < \sigma_1 < 2.55$), with a high positive asymmetry ($0.27 < sk_1 < 0.75$). On the CM diagram, they correspond to uniform suspension (fig. 5). Compact silts usually occur where the alluvial floor is eroded and incised into older Holocene floodplain deposits. In these floodplain remnants, the cohesion of silty material (resistance measured by penetration test = 25-35 KPa) forms resistant channel boundaries. Zones of enhanced erosion may take the form of small sub-circular depressions ($\varnothing = 30-70$ cm; depth = 10-20 cm) that have been scoured



in the alluvial floor (photo 1E). These substrate irregularities probably record differential erosion caused by heterogeneities in sediment cohesion, porosity and/or permeability. They can result from both cavitation and abrasion processes caused by a combination of flow turbulence and effects of shock waves. Examples of these processes have been described by E.E. Wohl (1999, p. 199), who indicates that "an initial substrate irregularity may perturb flow and sediment movement, initiating turbulence and cavitation which lead to differential erosion of the substrate".

River mouth mud beds

Mudbeds at river mouths, with a thickness that generally does not exceed 0.6 m, cover both sand beds and compact silts. They consist of sandy silt and clayey silt with a median grain size (D_{50}) from 0.077 mm to 0.019 mm (fig. 4F and 4G). The CM diagram records mixed transport processes, including dominant uniform suspension with incorporation of some grains transported by graded suspension during flood events (fig. 5). These deposits are consequently very poorly sorted, with a typical standard deviation of 2.20 to 2.23. The skewness of all the samples shows a positive value, ranging from 0.26 to 0.71. Mouth mud beds contain some marine

Fig. 5 – CM diagram (after R. Passega, 1957) of channel deposits in the Grand Rhône and the Petit Rhône.

Fig. 5 – Image granulométrique CM de R. Passega (1957) des dépôts de fond des chenaux du Grand Rhône et du Petit Rhône.

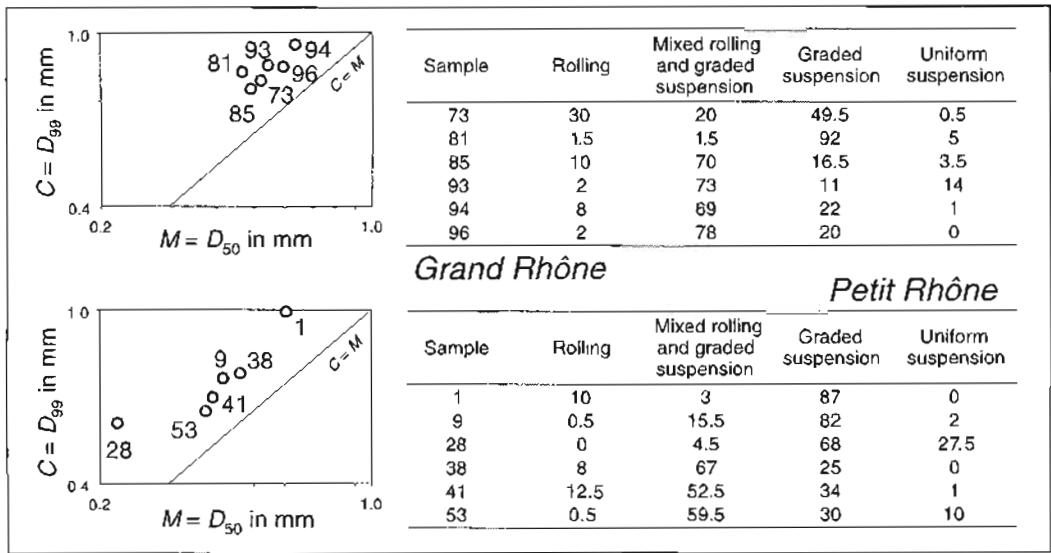
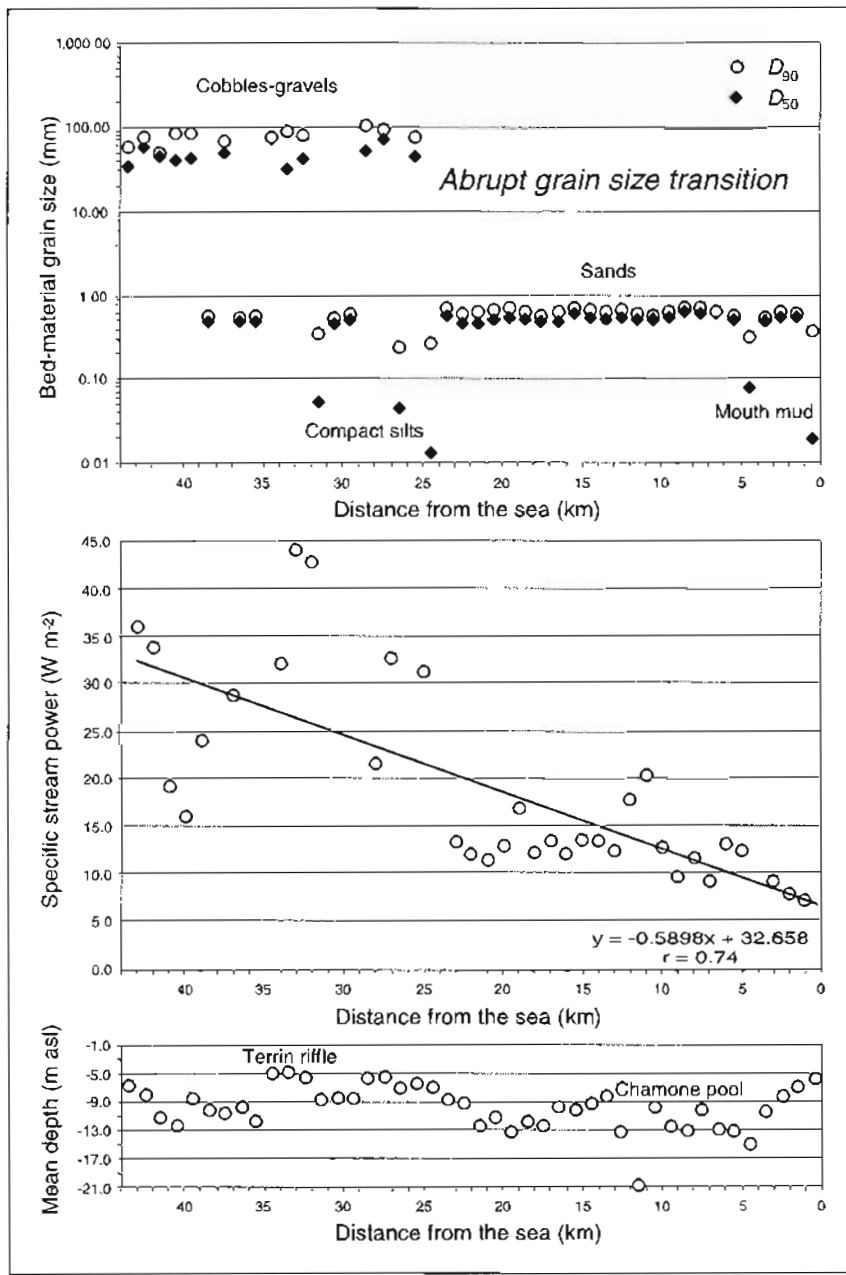


Fig. 6 – Quantification of transport modes for the sand fraction in the Grand Rhône and the Petit Rhône using the G.S. Visher (1969) method (values in percentages).

Fig. 6 – Quantification des modes de transport de la fraction sableuse du Grand Rhône et du Petit Rhône par la méthode de G.S. Visher (1969) (valeurs en pourcentages).



species, especially *Tellina planata* and *Serpula*. The muds, located exclusively near the river mouth, are derived by clay flocculation induced by incursion of marine water in the channel bottom during periods of low flow (Savey et al., 1971; Carrio, 1988).

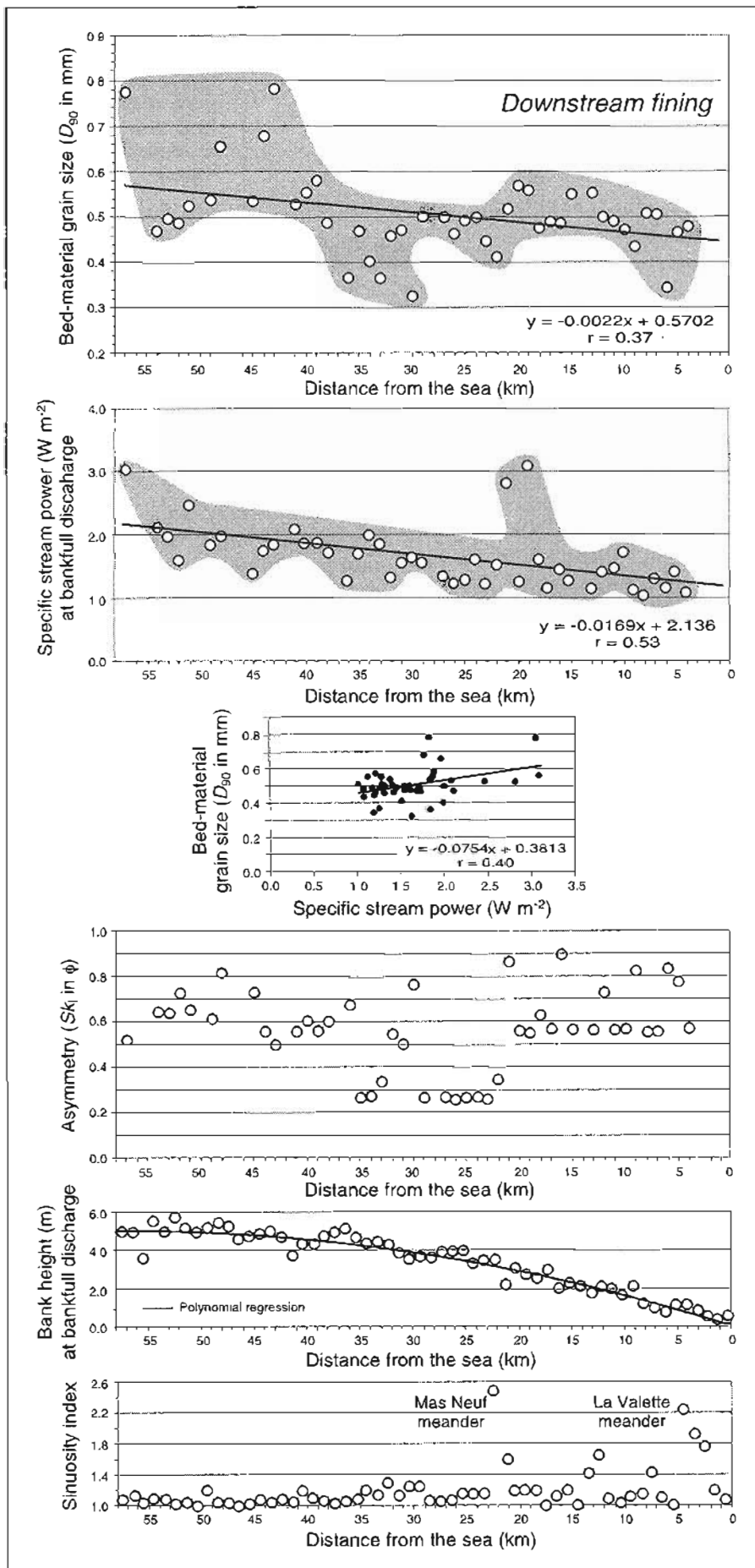
Gravel-sand transition and downstream fining in river sand beds

Bed material in both Rhône Delta river channels becomes systematically finer downstream of the deltaic diffluence, also downstream fining is different in the two distributaries.

In the Grand Rhône, bed-material is mainly gravel-sand dominated in the upstream section ($D_{90} = 57.6$ mm; $D_{50} = 34$ mm), and becomes sand-dominated further downstream, with lower values near the river mouth ($D_{90} = 0.78$ mm; $D_{50} = 0.55$ mm). The longitudinal profile of bed-material grain size shows a gravel-sand transition between the cobble-pebble beds and the dominant sand beds (fig. 7). As indicated by G.H. Sambrook Smith and R.I. Ferguson (1995), three possible

Fig. 7 – Downstream change in grain size, mean depth and specific stream power in the Grand Rhône. Symbols D_{90} and D_{50} refer to maximum bed-material grain size and median bed-material grain size, respectively.

Fig. 7 – Évolution longitudinale de la granulométrie du matériel de fond, de la profondeur moyenne et de la puissance spécifique du Grand Rhône. Les symboles D_{90} et D_{50} correspondent respectivement à la taille maximale et à la médiane du matériel de fond.

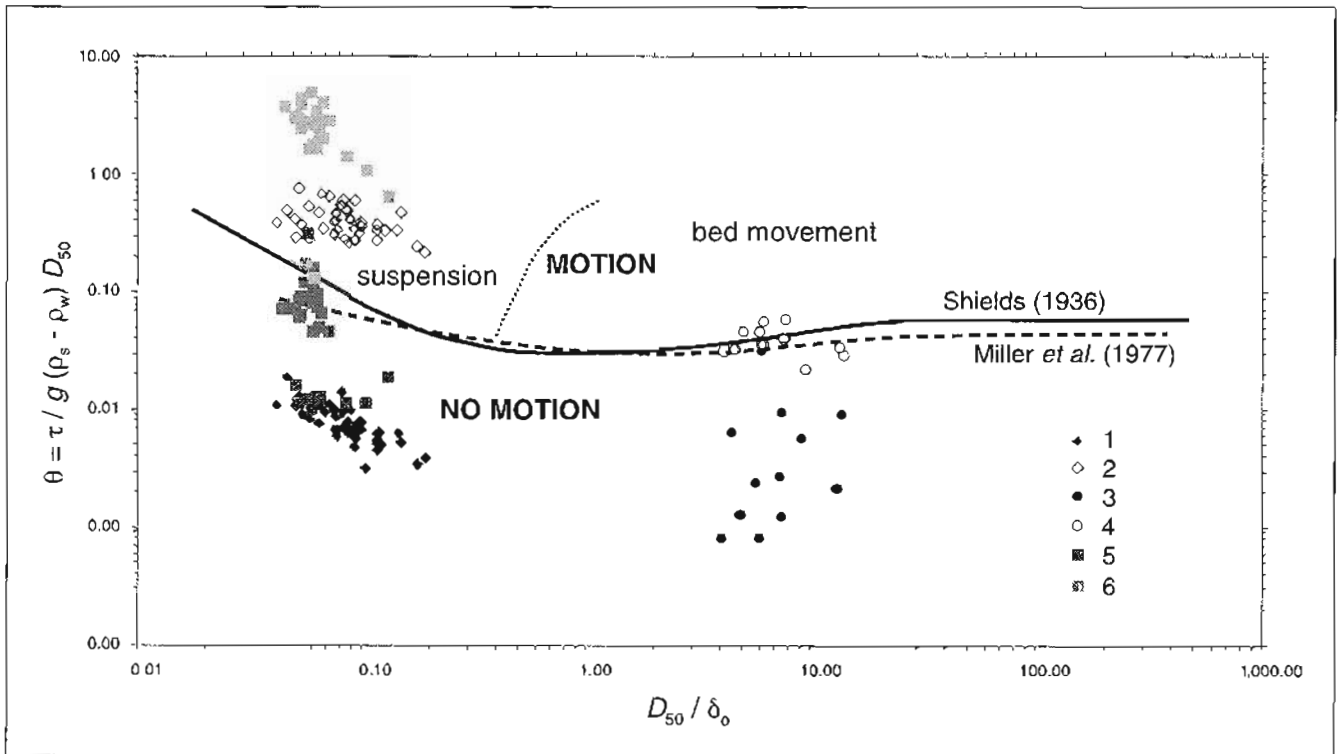


mechanisms may explain such a transition: local base-level control, excess of sand supply, or abrasion/breakdown of fine gravel. In the Grand Rhône, we explain the gravel-sand transition at 25 km upstream of the river mouth by two major factors: (1) inherited cobbles-pebbles derived from the Durancian Pleistocene substrate or Holocene marine shingle bars disappear downstream, and (2) slope rapidly reduces (*i.e.*, from 0.0003 m m⁻¹ to 0.00011 m m⁻¹), that inhibits the potential transport of both cobbles and pebbles. Thus, downstream of the 25 km point, median bed-material grain size (D_{50}) decreases rapidly from 45-70 mm to less than 0.65 mm within a few kilometres. Decreasing bed-material grain size and reduction of energy slope are accompanied by decreased specific stream power (*i.e.*, from 43.87-16.10 W m⁻² to 20.32-7.18 W m⁻² at bankfull discharge).

In the Petit Rhône, the longitudinal profile of maximum bed-material grain size (D_{90}) is characterised by high dispersion of values, regardless of distance from the river mouth (fig. 8). However, three distinct sections are distinguished. (1) The upper section of the Petit Rhône (*i.e.*, from the difffluence to the 43 km point) is characterised by the occurrence of the coarsest sand beds ($D_{90} = 0.78$ mm). Specific stream power values ($2.46 \text{ W m}^{-2} < \omega < 3.04 \text{ W m}^{-2}$), which are high immediately downstream of the difffluence, explains this observations. Then, with increasing distance from the difffluence, the specific stream power rapidly decreases (reduction of ~40% in 12 km). This phenomenon, combined with low water slope, induces a selective transport that causes the deposition of the

Fig. 8 – Downstream change in grain size, specific stream power, water slope and sinuosity of the Petit Rhône. Symbol D_{90} refers to the maximum bed-material grain size.

Fig. 8 – Évolution longitudinale de la granularité du matériel de fond, de la puissance spécifique, de la pente de la ligne d'eau et de la sinuosité du Petit Rhône. Le symbole D_{90} correspond à la taille maximale du matériel de fond.



coarsest sand fraction. This section is also characterised by the highest variability of maximum grain size ($0.47 \text{ mm} < D_{90} < 0.78 \text{ mm}$; mean 0.6 mm), due to the heterogeneity of the surveyed sites (alternation of large-shallow-straight and narrow-deep-sinuuous channel sections). In addition, high positive asymmetry values ($0.50 < sk_1 < 0.81$) indicate the predominance of fine particles (*i.e.*, clayed silt deposited during flood recession). To summarise, this upper section is characterised by storage of both coarse sand and fine silt in low-energy sections. (2) Grain-size variations between the 43 km and the 23 km points are lower and the maximum grain size is finer ($0.33 \text{ mm} < D_{90} < 0.58 \text{ mm}$; mean 0.46 mm), involving more gentle and regular hydrodynamics. This is correlated primarily specific stream power, which is less important and less fluctuant ($1.20 \text{ W m}^{-2} < \omega < 2.07 \text{ W m}^{-2}$), and also with storage of coarsest sand in low-energy sections upstream of the 43 km point. In some sections (36-34 km points; 30-23 km points), the percentage of fine grains is low ($0.25 < sk_1 < 0.33$) due to entrainment of silt particles by fluvial sorting process. In other sections (46-37 km points; 33-31 km points; 22 km point), the presence of sediments with high positive asymmetry values ($0.50 < sk_1 < 0.86$) characterises areas dominated by storage of fine particles. (3) From the 23 km point to the river mouth, maximum grain size records a slight increase ($0.34 \text{ mm} < D_{90} < 0.57 \text{ mm}$; mean 0.49 mm). One possible explanation may be that local specific stream power increases between the 22 km and the 20 km points. In any case, maximum values of D_{90} remain lower than those mentioned above at the beginning of the previous section. Moreover, downstream fining seems to occur at this section. Upstream, D_{90} is about 0.57 mm ; near the river mouth, values tend to become finer ($\sim 0.48 \text{ mm}$). Downstream fining, which results from repetitive phases of deposition of the coarsest sand, is explained here by significant

Fig. 9 – The Shields diagram (modified by M.C. Miller *et al.*, 1977) as a tool for estimate bed-material motion in the Grand Rhône and Petit Rhône. 1: Petit Rhône River at low flow (sand); 2: Petit Rhône River at bankfull discharge (sand); 3: Grand Rhône River at low flow (cobble-pebble); 4: Grand Rhône River at bankfull discharge (cobble-pebble); 5: Grand Rhône River at low flow (sand); 6: Grand Rhône River at bankfull discharge (sand).

Fig. 9 – Le diagramme de Shields (modifié par M.C. Miller *et al.*, 1977), utilisé comme outil de reconnaissance pour l'estimation des seuils critiques de mise en mouvement du matériel de fond dans le Grand Rhône et le Petit Rhône. 1 : Petit Rhône en période de basses eaux (sables) ; 2 : Petit Rhône lors du débit de pleins bords (sables) ; 3 : Grand Rhône en période de basses eaux (galets) ; 4 : Grand Rhône lors du débit de pleins bords (galets) ; 5 : Grand Rhône en période de basses eaux (sables) ; 6 : Grand Rhône lors du débit de pleins bords (sables).

specific stream power decrease ($3.08 \text{ W m}^{-2} > \omega > 1.01 \text{ W m}^{-2}$) and increase of channel sinuosity (fig. 8). In addition, high positive asymmetry values ($0.55 < sk_1 < 0.90$) characterise the predominance of fine grains in the deposit. The fine particles correspond to silt supplied by the river during flood events and/or, further downstream, to clay flocculated in presence of the salt tongue in the river channel. Thus, downstream fining, combined with numerous possibilities of deposition in meanders and the presence of a salt wedge, induce significant sediment storage in the lower section of the Petit Rhône.

Relationship of bed-material grain size to shear stress, stream power and transport capacity

A scatter plot of median grain size *versus* bed shear stress serves to identify the critical threshold of transport and deposition in the Rhône River during low water flow and bankfull discharge (fig. 9).

A	Q_{LF} $m^3 s^{-1}$	D_{50} mm	d m	ω $W m^{-2}$	ω_0 $W m^{-2}$	i_b $kg m^{-1} s^{-1}$
100		0.05	3.91	0.012	0.006	0.00005
		0.08	3.91	0.012	0.012	0.00000

B	Q_b $m^3 s^{-1}$	D_{50} mm	d m	ω $W m^{-2}$	ω_0 $W m^{-2}$	i_b $kg m^{-1} s^{-1}$
600		0.20	6.69	1.94	0.05	0.104
		0.25	6.69	1.94	0.07	0.091
		0.30	6.69	1.94	0.09	0.082
		0.35	6.69	1.94	0.11	0.075
		0.40	6.69	1.94	0.13	0.069
		0.45	6.69	1.94	0.15	0.063
		0.50	6.69	1.94	0.18	0.059
		0.55	6.69	1.94	0.20	0.055
		0.60	6.69	1.94	0.23	0.051
		2.72	6.69	1.94	1.94	0.000

C	Q_{LF} $m^3 s^{-1}$	D_{50} mm	d m	ω $W m^{-2}$	ω_0 $W m^{-2}$	i_b $kg m^{-1} s^{-1}$
900		0.35	6.83	0.39	0.11	0.005
		0.40	6.83	0.39	0.13	0.004
		0.45	6.83	0.39	0.15	0.003
		0.50	6.83	0.39	0.18	0.002
		0.55	6.83	0.39	0.20	0.002
		0.60	6.83	0.39	0.23	0.001
		0.87	6.83	0.39	0.39	0.000

D	Q_{LF} $m^3 s^{-1}$	D_{50} mm	d m	ω $W m^{-2}$	ω_0 $W m^{-2}$	i_b $kg m^{-1} s^{-1}$
900	30.00 to 80.00		5.02	5.41	51.46 to 199.88	No transport

E	Q_{LF} $m^3 s^{-1}$	D_5 mm	d m	ω $W m^{-2}$	ω_0 $W m^{-2}$	i_b $kg m^{-1} s^{-1}$
900	10.00 to 50.00		5.02	5.41	11.61 to 105.70	No transport

F	Q_b $m^3 s^{-1}$	D_{50} mm	d m	ω $W m^{-2}$	ω_0 $W m^{-2}$	i_b $kg m^{-1} s^{-1}$
5400		0.35	9.27	12.54	0.11	1.052
		0.40	9.27	12.54	0.13	0.981
		0.45	9.27	12.54	0.16	0.922
		0.50	9.27	12.54	0.18	0.872
		0.55	9.27	12.54	0.21	0.829
		0.60	9.27	12.54	0.24	0.791
		10.04	9.27	12.54	12.54	0.000

G	Q_b $m^3 s^{-1}$	D_{50} mm	d m	ω $W m^{-2}$	ω_0 $W m^{-2}$	i_b $kg m^{-1} s^{-1}$
5400	30.00 to 80.00		9.05	31.72	56.78 to 217.66	No transport

H	Q_b $m^3 s^{-1}$	D_5 mm	d m	ω $W m^{-2}$	ω_0 $W m^{-2}$	i_b $kg m^{-1} s^{-1}$
5400		10.00	9.05	30.14	12.39	0.343
		15.00	9.05	30.14	21.77	0.091
		18.97	9.05	30.14	30.14	0.000

During periods of low water flow, the results (using the Shields diagram) suggest that the sand fraction cannot be displaced at its contact with the bed of the Petit Rhône. In the Grand Rhône, most of the sand fraction cannot be moved at low flow, but higher bed shear stress may initiate selective entrainment of the finest particles near the channel bottom. According to the Shields diagram, displacement of the sand fraction may be due to suspension process. However, involvement of rolling process in the displacement of the sand fraction also appears by the presence of small sigmoidal and asymmetric sand ridges on the channel floor. The cobble-pebble fraction cannot be displaced during low water because of insufficient flow velocity.

In contrast, sand motion may be common at bankfull discharge. The Shields diagram (fig. 9) indicates that transport of sand particles is dominated by suspension; the CM diagram of Passega (fig. 5) further suggests that mixed (graded) suspension process and rolling process are not excluded. Moreover, higher bed shear stress results in the movement of the finest cobble-pebble fraction by rolling process. The basic problem remains as to the bed-material transport capacity under different conditions of low flow and bankfull discharge.

Critical stream power values (estimated using eq. 5) to entrain sediment of different size are given in table 3. These indicate that

Table 3 – Estimated critical stream power (ω_0) and specific bed-material transport rate (i_b). A: during low water flow on the Petit Rhône; B: during bankfull discharge on the Petit Rhône; C: during low water flow in low slope sections of the Grand Rhône; D: during low water flow in high slope sections of the Grand Rhône (D_{50}); E: during low water flow in high slope sections of the Grand Rhône ($D_5 = 5$ th percentile); F: during bankfull discharge in low slope sections of the Grand Rhône; G: during bankfull discharge in high slope sections of the Grand Rhône (D_{50}); H: during bankfull discharge in high slope sections of the Grand Rhône ($D_5 = 5$ th percentile).

Tableau 3 – Estimation des puissances spécifiques critiques (ω_0) et des taux de transport unitaires de la charge de fond (i_b). A : en période de basses eaux dans le Petit Rhône ; B : lors du débit de pleins bords dans le Petit Rhône ; C : en période de basses eaux dans les tronçons de faible énergie du Grand Rhône ; D : en période de basses eaux dans les tronçons de forte énergie du Grand Rhône (D_{50}) ; E : en période de basses eaux dans les tronçons de forte énergie du Grand Rhône ($D_5 = 5^e$ percentile) ; F : lors du débit de pleins bords dans les tronçons de faible énergie du Grand Rhône ; G : lors du débit de pleins bords dans les tronçons de forte énergie du Grand Rhône (D_{50}) ; H : lors du débit de pleins bords dans les tronçons de forte énergie du Grand Rhône ($D_5 = 5^e$ percentile).

tion at 25 km upstream of the Grand Rhône river mouth. In the Petit Rhône, cobble-pebble beds are rare because specific stream power is too low to provide traction processes.

6) The drastic reduction of the bed-material volume, since the end of the Little Ice Age, induced by decreased runoff and increased channelisation, dam construction, dredging and mining, has generated a serious sand deficit in the Rhône Delta. Both channels are particularly vulnerable to this sand deficit since most of the fluvial beds are composed by sands. Present hydraulic attributes, such as high specific stream power, explain the presence of numerous and different incised channel sections that create a bed-material *discontinuum* in the Grand Rhône and Petit Rhône.

Acknowledgements

We express our gratitude to the Compagnie Nationale du Rhône (CNR) for providing hydraulic data. We also acknowledge Michel Guillemard (CETE Méditerranée) for his assistance with core sampling and for channel photographs. Pierre Freydet (University of Paris-Orsay) for identification of benthic macroinvertebrate species, Didier Jézéquel (University of Paris 7 Denis-Diderot) for water electric conductivity measurements, and Luc Long (DRAASM, Marseilles) who kindly lent us subaquatic archaeological photographs. The earlier version of the text benefited from perceptive reviews by Jean-Paul Bravard (University of Lyon 2), Mireille Provansal (University of Aix-Marseille 1) and two anonymous reviewers. Thanks to the Editorial Board of the journal, and special thanks to Daniel Jean Stanley (Smithsonian of Washington) for verifying the English language of the manuscript.

References

- Antonelli C. (2002) – Flux sédimentaires et morphogénèse récente dans le chenal du Rhône aval. Thèse en géographie physique, Université Aix-Marseille 1, 279 p.
- Arnaud-Fassetta G. (1996) – Les inondites rhodaniennes d'octobre 1993 et janvier 1994 en milieu fluvio-deltaïque. L'exemple du Petit Rhône. *Quaternaire*, 7, 2, 139-153.
- Arnaud-Fassetta G. (1997) – Évolution du plancher alluvial du Petit Rhône à l'échelle pluriannuelle (delta du Rhône, France du Sud). *Géomorphologie : Relief, Processus, Environnement*, 3, 237-256.
- Arnaud-Fassetta G. (1998) – *Dynamiques fluviales holocènes dans le delta du Rhône*. Presses Universitaires du Septentrion, Lille, 329 p.
- Arnaud-Fassetta G. (2000) – *Quatre mille ans d'histoire hydrologique dans le delta du Rhône. De l'Âge du Bronze au siècle du nucléaire*. Grafigéo, 11, Collection mémoires et documents de l'UMR PRODIG, Paris, 229 p.
- Arnaud-Fassetta G. (2003) – River channel changes in the Rhone Delta (France) since the end of the Little Ice Age: geomorphological adjustment to hydroclimatic change and natural resource management. *Catena*, 51, 2, 141-172.
- Bagnold R.A. (1966) – An approach to the sediment transport problem from general physics. *United States Geological Survey Professional Paper*, 422-I, 1-37.
- Bagnold R.A. (1980) – An empirical correlation of bedload transport rates in flumes and natural rivers. *Proceedings of the Royal Society*, 372A, 453-473.
- Bathurst J.C., Graf W.H., Cao H.H. (1987) – Bed load discharge equations for steep mountain rivers. In Thorne C.R., Bathurst J.C., Hey R.D. (Eds.) *Sediment transport in gravel-bed rivers*. John Wiley and Sons, Chichester, 453-491.
- Bravard J.P., Peiry J.L. (1999) – The CM pattern as a tool for the classification of alluvial suites and floodplains along the river continuum. In Marriott S.B., Alexander J. (Eds.) *Floodplains: Interdisciplinary Approaches*. Geological Society, London, Special Publications, 163, 259-268.
- Carrio C. (1988) – *Contribution à l'étude dynamo-sédimentaire du delta rhodanien et du processus d'émergence de la plaine deltaïque associée (exemple de La Palissade, Camargue, France)*. Thèse, Université Aix-Marseille-1, 359 p.
- Church M.A., McLean D.G., Wolcott J.F. (1987) – River bed gravels: sampling and analysis. In Thorne C.R., Bathurst J.C., Hey R.D. (Eds.) *Sediment Transport in Gravel-Bed Rivers*. John Wiley and Sons, Chichester, 43-88.
- Doyle M.W., Shields Jr. F.D. (2000) – Incorporation of bed texture into a channel evolution model. *Geomorphology*, 34, 291-309.
- Dugas F. (1989) – *Étude du transit sédimentaire par charriage dans le Rhône entre Beaucaire et Arles*. Institut Français de Recherche Scientifique pour le Développement en Coopération et Compagnie Nationale du Rhône, Montpellier, 65 p.
- Ferguson R.J., Hoey T., Wathen S., Werritty A. (1996) – Field evidence for rapid downstream fining of river gravels through selective transport. *Geology*, 24, 179-182.
- Folk R.L. (1980) – *Petrology of Sedimentary Rocks*. Hemphills, Austin, 182 p.
- Folk R.L., Ward W.C. (1957) – Brazos river bar: a study in the significance of grain size parameters. *Journal of Sedimentary Petrology*, 27, 3-26.
- Gilvear D., Bradley S. (1997) – Geomorphological adjustment of a newly engineered upland sinuous gravel-bed river diversion: Evan Water, Scotland. *Regulated Rivers: Research and Management*, 13, 377-389.
- Gomez B., Church M.A. (1989) – An assessment of bed load sediment transport formulae for gravel bed rivers. *Water Resources Research*, 25, 1161-1186.
- Ham D.G., Church M.A. (2000) – Bed-material transport estimated from channel morphodynamics: Chilliwack River, British Columbia. *Earth Surface Processes and Landforms*, 25, 1123-1142.
- Hensel P.F., Day Jr. J.W., Pont D. (1999) – Wetland vertical accretion and soil elevation change in the Rhône River Delta, France: the importance of riverine flooding. *Journal of Coastal Research*, 15, 3, 593-858.
- Hoey T.B., Bluck B.J. (1999) – Identifying the controls over downstream fining of river gravels. *Journal of Sedimentary Research*, 69, 40-50.
- Kellerhalls R., Church M.A., Bray D.I. (1976) – Classification and analysis of river processes. *Journal of the Hydraulics Division, American Society of Civil Engineers*, 102, 813-829.
- Knighton D. (1998) – *Fluvial forms and processes. A new perspective*. Arnold, London, 383 p.

tion at 25 km upstream of the Grand Rhône river mouth. In the Petit Rhône, cobble-pebble beds are rare because specific stream power is too low to provide traction processes.

6) The drastic reduction of the bed-material volume, since the end of the Little Ice Age, induced by decreased runoff and increased channelisation, dam construction, dredging and mining, has generated a serious sand deficit in the Rhône Delta. Both channels are particularly vulnerable to this sand deficit since most of the fluvial beds are composed by sands. Present hydraulic attributes, such as high specific stream power, explain the presence of numerous and different incised channel sections that create a bed-material *discontinuum* in the Grand Rhône and Petit Rhône.

Acknowledgements

We express our gratitude to the Compagnie Nationale du Rhône (CNR) for providing hydraulic data. We also acknowledge Michel Guillemard (CETE Méditerranée) for his assistance with core sampling and for channel photographs. Pierre Freydet (University of Paris-Orsay) for identification of benthic macroinvertebrate species, Didier Jézéquel (University of Paris 7 Denis-Diderot) for water electric conductivity measurements, and Luc Long (DRAASM, Marseilles) who kindly lent us subaquatic archaeological photographs. The earlier version of the text benefited from perceptive reviews by Jean-Paul Bravard (University of Lyon 2), Mireille Provansal (University of Aix-Marseille 1) and two anonymous reviewers. Thanks to the Editorial Board of the journal, and special thanks to Daniel Jean Stanley (Smithsonian of Washington) for verifying the English language of the manuscript.

References

- Antonelli C. (2002) – Flux sédimentaires et morphogénèse récente dans le chenal du Rhône aval. Thèse en géographie physique, Université Aix-Marseille 1, 279 p.
- Arnaud-Fassetta G. (1996) – Les inondites rhodaniennes d'octobre 1993 et janvier 1994 en milieu fluvio-deltaïque. L'exemple du Petit Rhône. *Quaternaire*, 7, 2, 139-153.
- Arnaud-Fassetta G. (1997) – Évolution du plancher alluvial du Petit Rhône à l'échelle pluriannuelle (delta du Rhône, France du Sud). *Géomorphologie : Relief, Processus, Environnement*, 3, 237-256.
- Arnaud-Fassetta G. (1998) – *Dynamiques fluviales holocènes dans le delta du Rhône*. Presses Universitaires du Septentrion, Lille, 329 p.
- Arnaud-Fassetta G. (2000) – *Quatre mille ans d'histoire hydrologique dans le delta du Rhône. De l'Âge du Bronze au siècle du nucléaire*. Grafigéo, 11, Collection mémoires et documents de l'UMR PRODIG, Paris, 229 p.
- Arnaud-Fassetta G. (2003) – River channel changes in the Rhone Delta (France) since the end of the Little Ice Age: geomorphological adjustment to hydroclimatic change and natural resource management. *Catena*, 51, 2, 141-172.
- Bagnold R.A. (1966) – An approach to the sediment transport problem from general physics. *United States Geological Survey Professional Paper*, 422-1, 1-37.
- Bagnold R.A. (1980) – An empirical correlation of bedload transport rates in flumes and natural rivers. *Proceedings of the Royal Society*, 372A, 453-473.
- Bathurst J.C., Graf W.H., Cao H.H. (1987) – Bed load discharge equations for steep mountain rivers. In Thorne C.R., Bathurst J.C., Hey R.D. (Eds.) *Sediment transport in gravel-bed rivers*. John Wiley and Sons, Chichester, 453-491.
- Bravard J.P., Peiry J.L. (1999) – The CM pattern as a tool for the classification of alluvial suites and floodplains along the river continuum. In Marriott S.B., Alexander J. (Eds.) *Floodplains: Interdisciplinary Approaches*. Geological Society, London, Special Publications, 163, 259-268.
- Carrio C. (1988) – *Contribution à l'étude dynamo-sédimentaire du delta rhodanien et du processus d'émergence de la plaine deltaïque associée (exemple de La Palissade, Camargue, France)*. Thèse, Université Aix-Marseille-1, 359 p.
- Church M.A., McLean D.G., Wolcott J.F. (1987) – River bed gravels: sampling and analysis. In Thorne C.R., Bathurst J.C., Hey R.D. (Eds.) *Sediment Transport in Gravel-Bed Rivers*, John Wiley and Sons, Chichester, 43-88.
- Doyle M.W., Shields Jr. F.D. (2000) – Incorporation of bed texture into a channel evolution model. *Geomorphology*, 34, 291-309.
- Dugas F. (1989) – *Étude du transit sédimentaire par charriage dans le Rhône entre Beaucaire et Arles*. Institut Français de Recherche Scientifique pour le Développement en Coopération et Compagnie Nationale du Rhône, Montpellier, 65 p.
- Ferguson R.J., Hoey T., Wathen S., Werritty A. (1996) – Field evidence for rapid downstream fining of river gravels through selective transport. *Geology*, 24, 179-182.
- Folk R.L. (1980) – *Petrology of Sedimentary Rocks*. Hemphills, Austin, 182 p.
- Folk R.L., Ward W.C. (1957) – Brazos river bar: a study in the significance of grain size parameters. *Journal of Sedimentary Petrology*, 27, 3-26.
- Gilvear D., Bradley S. (1997) – Geomorphological adjustment of a newly engineered upland sinuous gravel-bed river diversion: Evan Water, Scotland. *Regulated Rivers: Research and Management*, 13, 377-389.
- Gomez B., Church M.A. (1989) – An assessment of bed load sediment transport formulae for gravel bed rivers. *Water Resources Research*, 25, 1161-1186.
- Ham D.G., Church M.A. (2000) – Bed-material transport estimated from channel morphodynamics: Chilliwack River, British Columbia. *Earth Surface Processes and Landforms*, 25, 1123-1142.
- Hensel P.F., Day Jr. J.W., Pont D. (1999) – Wetland vertical accretion and soil elevation change in the Rhône River Delta, France: the importance of riverine flooding. *Journal of Coastal Research*, 15, 3, 593-858.
- Hoey T.B., Bluck B.J. (1999) – Identifying the controls over downstream fining of river gravels. *Journal of Sedimentary Research*, 69, 40-50.
- Kellerhalls R., Church M.A., Bray D.I. (1976) – Classification and analysis of river processes. *Journal of the Hydraulics Division, American Society of Civil Engineers*, 102, 813-829.
- Knighton D. (1998) – *Fluvial forms and processes. A new perspective*. Arnold, London, 383 p.

- L'Homer A. (1987) – *Notice explicative de la carte géologique d'Arles au 1/50000*. BRGM, Orléans, 72 p.
- Lane E.W. (1955) – Design of stable channels. *Transactions of the American Society of Civil Engineers*, 120, 1234-1260.
- Martin Y., Church M.A. (2000) – Re-examination of Bagnold's empirical bedload formulae. *Earth Surface Processes and Landforms*, 25, 1011-1024.
- Miller M.C., McCave I.N., Komar P.D. (1977) – Threshold of sediment motion under unidirectional currents. *Sedimentology*, 24, 507-527.
- Pardé M. (1925) – *Le régime du Rhône. Étude hydrologique*. Première partie, Étude générale. Institut des Études Rhodaniennes, Université de Lyon. Masson, Paris, 883 p.
- Passega R. (1957) – Texture as characteristic of clastic deposition. *American Association of Petroleum Geologists Bulletin*, 41, 1952-1964.
- Pauc H.E. (1976) – Comportement dynamique des matériaux en suspension. Étude de divers secteurs côtiers du Golfe du Lion. *Bulletin de la Société d'Histoire naturelle d'Afrique du Nord*, 67, 151-169.
- Pont D. (1992) – *Caractérisation de la charge en suspension du Rhône au niveau du palier d'Arles lors d'une crue importante*. Rapport final du groupe de travail "Apports à la Méditerranée", Agence de l'eau Rhône-Méditerranée-Corse. Laboratoire de biologie animale et d'écologie, Écologie des systèmes fluviaux, Arles, 25 p.
- Pont D., Simmonet J.P., Walter A.V. (2002) – Medium-term changes in suspended sediment delivery to the ocean: consequences of catchment heterogeneity and river management (Rhône River, France). *Estuarine, Coastal and Shelf Sciences*, 54, 1-18.
- Quisserne D. (2000) – *Caractérisation de la charge de fond du Rhône dans son aire deltaïque*. Hydrologie-sédimentologie-écologie. Mémoire de maîtrise en géographie physique, Université Paris-7 Denis-Diderot, 143 p.
- Rice S. (1999) – The nature and controls on downstream fining within sedimentary links. *Journal of Sedimentary Research*, 69, 32-39.
- Roditis J.C. (1993) – *Caractérisation de la charge solide en suspension et alluvionnement du Rhône dans le secteur Beaucaire-Arles. Crues et modalités du transfert sédimentaire. Bilan actuel et évolution récente*. Mémoire de DEA, Université Aix-Marseille I, 135 p.
- Sambrook Smith G.H., Ferguson R.I. (1995) – The gravel-sand transition along river channels. *Journal of Sedimentary Research*, 65, 423-430.
- Savey P., Pommier M., Marvaud P. (1971) – *Observations et mesures effectuées sur les coins salés du Grand et du Petit Rhône*. Compagnie Nationale du Rhône, Société Hydrotechnique de France, session 94 du Comité Technique, L'Hydraulique et les industries littorales, Lyon, 17 p.
- Shields A. (1936) – *Anwendung der Ähnlichkeitsmechanik und der Turbulenzforschung auf die Geschiebebewegung*. Mitteilungs der Preussischen Versuchsanstalt für Wasserbau und Schiffbau, 26, Berlin, 24 p.
- Suarez S. (1997) – *Dynamiques sédimentaires actuelles et récentes de la frange littorale orientale du delta du Rhône*. Thèse en géographie physique, Université Aix-Marseille I, 283 p.
- Suarez S., Provansal M. (1998) – Large scale evolution of the littoral of the Rhône Delta (Southeast France). *Journal of Coastal Research*, 14, 493-501.
- Surrell E. (1847) – *Mémoire sur l'amélioration des embouchures du Rhône*. Imprimerie cévenole, Nîmes, 8 p.
- Van Straaten L.M.J.U. (1959) – Littoral and submarine morphology of the Rhône delta. In Russell R.J. (Ed.), *Second Coastal Geography Conference Baton Rouge Proceedings*. Geography Branch, Office of Naval Research, Washington D.C., 233-264.
- Visher G.S. (1969) – Grain size distributions and depositional processes. *Journal of Sedimentary Petrology*, 39, 1074-1106.
- Werrity A. (1992) – Downstream fining in a gravel-bed river in southern Poland: lithologic controls and the role of abrasion. In Billi P., Thorne C.R., Hey R.D., Tacconi P. (Eds.) *Dynamics of Gravel-bed Rivers*. John Wiley and Sons, Chichester, 251-272.
- Wohl E.E. (1999) – Incised bedrock channels. In Darby S.E., Simon A. (Eds.) *Incised River Channels. Processes, Forms, Engineering and Management*. John Wiley and Sons, Chichester, 187-218.

Article reçu le 18 février 2002, accepté le 13 mars 2003